# Chapter 8

# ON INCORPORATING PARASITIC QUANTUM EFFECTS IN CLASSICAL CIRCUIT SIMULATIONS

Frank Felgenhauer, Maik Begoin and Wolfgang Mathis

*University of Hannover, Institute of Electromagnetic Theory and Microwave Technique, Appelstraÿe 9A, 30167 Hannover, Germany*

E-mail: (felgenhauer, begoin, mathis)@tet.uni-hannover.de

**Abstract:** In this chapter, we present a discussion about the influence of parasitic quantum effects to the functionality of classical electronic circuit concepts. The discussion covers the physics and the simulation of coherent charge transport and also the way to include quantum effects in high level circuit simulators like SPICE. Electronic circuits we are talking about are scaled into a domain where the common semi-classical transport models loose more and more their validity. Therefore, we start with a review of the semi-classical semiconductor equations and their extensions to include quantum effects. Further, a derivation of the quantum transport equations for coherent electron transport is given, including a short summary of current methods to solve these equations. The Schrödinger-Poisson solver we use to calculate transport is presented in detail. At the end of the chapter we show three different circuit examples, which explicitly exhibit the influence of quantum effects to circuit functionality.

**Key words:** CMOS circuits; parasitic quantum effects; SPICE simulation

## Introduction

Although several new device concepts are considered in nanotechnology during the last decade industrial applications will be dominated by CMOS technology in the near future since very complex CMOS circuits can be realized. Due to the rapid process of down-scaling of integrated semiconductor devices

*W. Grabinski, B. Nauwelaers and D. Schreurs (eds.),*
*Transistor Level Modeling for Analog/RF IC Design,* 209–241.
© 2006 *Springer. Printed in the Netherlands.*

the performance of a CMOS device is influenced by an increasing number of parasitic effects. Beside semi-classical parasitic effects and leakage currents such as sub-threshold currents, DIBL and GIBL [1] that have already taken into account in the sub-μm regime further parasitic effects of quantum mechanical origin must be included in device modelling. One of the well-known quantum mechanical effects is the tunneling current through thin potential barriers. For example, in 0.12 μm technology the oxide thicknesses of gates is below 3 nm and the direct tunneling current starts to increase exponentially [2, 3]. In consequence, for classical CMOS circuits we have to expect at least a dramatic increase of these parasitic currents leading to unacceptable noise levels in analog applications [4] and may even cause a failure of the circuit functionality [5]. However, there are more quantum mechanical phenomena, like charge quantization, scattering etc., which can restrict the functionality of classical circuits. In this chapter, we present our methodology to analyze nanoscaled circuits, from the physics of charge carrier transport to high-level, SPICE-like circuit simulators. We start the first section with a discussion of semi-classical semiconductor equations and their limits, when devices and structures in the mesoscopic regime are considered. Subsequent, we show a structural derivation of basic quantum transport equations in multi-layered semiconductors, since circuit designers are usually not familiar with physics of charge carrier transport in-depth. This section ends with a short summary about methods to solve the semi-classical and quantum mechanical semiconductors equations. In the following two sections we present in detail a self-consistent Schrödinger Poisson solver based on the non-equilibrium Green's function formalism (NEGF) and a Newton-Raphson algorithm. As an example, the calculation of coherent transport through isolating oxide layer, which corresponds to gate direct tunneling in MOSFET, is shown. Let us note at this point that the transport processes we consider in this chapter are all coherent since the considered nanoscaled devices and structures below 20 nm are much shorter than the coherence length. However, the algorithm we use to solve the Schrödinger equation (e.g. the NEGF formalism) can be extended to incoherent transport.

The last section is about the incorporation of the results of the quantum mechanical transport simulations into a high-level circuit simulator. We present three different circuit examples, each representing a specific circuit type and each example exhibits the influence of direct tunneling currents to the circuit functionality.

## 1. From Drift-Diffusion to Wavelike Behaviour

Devices in electronic circuits are connected to at least two contacts, therefore any device we are talking about is an open system with respect of charge carrier transport. In principle, transport processes in conductors and semiconductors

have to be described as many-body problems where the dynamics of particles have to be considered by an "ensemble" description instead of a single particle description or "test particle" description. This can be done for classical as well as quantum mechanical transport processes.

## 1.1. Semi-classical Transport

Classical transport processes are based on the classical Newton mechanics where we replace the single particle dynamics with the force $\mathbf{F} : I\!R^3 \to I\!R^3$ by the dynamics of a whole set of single particles which can be interpreted as an "ensemble" of particles. For this purpose we define a time-dependent probability distribution function $f(\mathbf{r}, \mathbf{v}, t)$ on the "state space" $(\mathbf{r}, \mathbf{v}) \in I\!R^3 \times I\!R^3$ of a one-particle system where $\mathbf{v}$ is the velocity of the particles and study their dynamics. Using $f(\mathbf{r}, \mathbf{v}, t)$ the number of particles at time $t$ in a volume $V$ can be calculated as

$$N(t) := \int f(\mathbf{r}, \mathbf{v}, t)\, d^3r d^3v. \tag{1}$$

The number of particles in $V$ changes with $t$ because some particles enter as well as leave $V$. At first we assume that there are no collisions between the particles. Then if a single particle is in a state $(\mathbf{r}, \mathbf{v})$ at time $t$ it will be in the state $(\mathbf{r} + \mathbf{v}\delta t, \mathbf{v} + (\mathbf{F}/m)\delta t)$. However we have

$$f\left(\mathbf{r} + \mathbf{v}\delta t, \mathbf{v} + \frac{\mathbf{F}}{m}\delta t, t + \delta t\right) = f(\mathbf{r}, \mathbf{v}, t). \tag{2}$$

If collisions occur an additional collision term has to be taken into account

$$f\left(\mathbf{r} + \mathbf{v}\delta t, \mathbf{v} + \frac{\mathbf{F}}{m}\delta t, t + \delta t\right) = f(\mathbf{r}, \mathbf{v}, t) + \left(\frac{\partial f}{\partial t}\right)_{\text{coll}} \delta t. \tag{3}$$

If the left hand side of (3) is to be developed to the first order we obtain *Boltzmann's equation* of kinetic theory (see e.g. Huang [6])

$$\left(\frac{\partial}{\partial t} + \mathbf{v} \cdot \nabla_r + + \frac{\mathbf{F}}{m} \cdot \nabla_v\right) f(\mathbf{r}, \mathbf{v}, t) = \left(\frac{\partial f}{\partial t}\right)_{\text{coll}}. \tag{4}$$

The second term of the left side of Eq. (4) is called *diffusion term* whereas the third term is called *drift term*. Note that Boltzmann's equation can be interpreted only if the collision term is defined explicitly.

If we restrict ourselves to two-particle interactions and molecular chaos is assumed an explicit collision term can be derived

$$\left(\frac{\partial f}{\partial t}\right)_{\text{coll}} = \int d\Omega \int d^3v_2 \sigma(\Omega) \|\mathbf{v}_1 - \mathbf{v}_2\| (f_2' f_1 - f_2 f_1) \tag{5}$$

where $\Omega$ is the angle between $\mathbf{v}_1 - \mathbf{v}_2$ and $\mathbf{v}_1' - \mathbf{v}_2'$, $f_1 := f(\mathbf{r}, \mathbf{v}_1, t), \ldots$ and $\sigma(\Omega)$ is the interaction cross-section and we obtain Boltzmann's famous transport equation. Conservation laws of transport processes can be derived if all terms of Boltzmann's equation weighted by a certain function $\Theta(\mathbf{r}, \mathbf{v})$ are averaged with respect to the velocity. Note that the corresponding average of the collision term is zero; see Huang [6] for further details. E.g. energy conservation can be derived if $\Theta$ is related to the kinetic energy $(1/2)mv^2$. Therefore a classical multi-body system can be described in a statistical manner by a distribution function $f(\mathbf{r}, \mathbf{v}, t)$ as a solution of Boltzmann's equation or by its moments that can be interpreted in a dynamical manner as conservation laws. The semi-classical transport theory of semiconductors can be developed quantitatively if a two-fluid model is used and distribution functions as well as Boltzmann's equations for electrons and holes are formulated and ad-hoc quantum mechanical assumptions will be added. If average processes are used we obtain the well-known van Roosbroeck equations or drift-diffusion model for the electron density $n$ and hole density $p$ of semiconductors (see e.g. van Roosbroeck [7], Selberherr [8])

$$\begin{aligned} \nabla \cdot (\varepsilon \nabla \varphi) &= -e(p - n + N_D^+ - N_A^-), \\ \frac{\partial n}{\partial t} &= \nabla \cdot (-\mu_n n \nabla \varphi + D_n \nabla n), \\ \frac{\partial p}{\partial t} &= \nabla \cdot (\mu_p p \nabla \varphi + D_p \nabla p) \end{aligned} \tag{6}$$

with $D_{n,p}$ as diffusion coefficients, $\mu_{n,p}$ as mobilities, and the donator density $N_D^+$ as well as the acceptor density $N_A^-$.

Unfortunately the relationship $(1/2)mv^2$ is not valid in quantum mechanics and a modification of the semi-classical Boltzmann equation is needed. There are different options to do this. In each case the drift term is modified.

A first modification of the Boltzmann equation was presented by Wigner in 1932 [9] who introduced a non-local potential $V$. Wigner transformed Boltzmann's equation with respect to the velocity $v$ into the $k$–space. Then the drift term is replaced by a memory term; in the 1-D case Wigner's variation of the Boltzmann equation can be formulated as

$$\frac{\partial f_w}{\partial t} = -\frac{\hbar k}{m}\frac{\partial f_w}{\partial x} - \frac{1}{\hbar}\int \frac{dk'}{2\pi} V(x, k - k') f_w(x, k, t) - \left(\frac{\partial f_w}{\partial t}\right)_{\text{coll}}, \tag{7}$$

where $f_w = f_w(x, k, t)$. Wigner's approach can be used for studying transport processes with quantum corrections. A first implementation for 1-D cases was presented by Biegel *et al.* [10] in the program SQUADS but a 2-D version of this program is not trivial (see Biegel [11]). An alternative concept for a Boltzmann equation with quantum corrections was presented by Nordheim [12] and Uhlenbeck [13].

A drift-diffusion model with quantum corrections was e.g. presented by Ancona [14]. Based on ideas of Madelung [15] and Bohm [16] originally introduced for an alternative interpretation of quantum mechanics Ancona added a quantum corrected potential ("Madelung-Bohm potential"). This model is denoted as "density-gradient model". Ancona's approach can be derived also from a quantum corrected variant so-called hydrodynamic approach that became popular in semiconductor device simulation during the last few years. Further details about quantum corrected hydrodynamical equations for semiconductor devices and its applications can be found in the literature, see e.g. [17], [18], [19], and others.

Another approach for the derivation of a quantum Boltzmann equation was given by Mahan [20] where the drift term was corrected, too. Mahan considered energy and impulse as independent variables and the modified distribution function is a solution of the following equation

$$\frac{\partial f}{\partial t} + \mathbf{v} \cdot \nabla_r f + \mathbf{F} \cdot \left( \frac{\nabla_v}{m} + \mathbf{v} \frac{\partial}{\partial \omega} \right) f = I(f), \tag{8}$$

with $I(f)$ as interaction term. Mahan's approach based on a certain Green function of a non-equilibrium system where the Keldysh formalism is used. An alternative derivation from first principles was presented recently by Prüstel [21]. His starting point is the Liouville-von-Neumann equation for the density matrix $\rho$ (see e.g. Mathis *et al.* [22]) $\dot{\rho} = i\mathcal{L}\rho$, where $\mathcal{L}$ is the so-called Liouville operator. Prüstel applied a decomposition of the density matrix $\rho$ into a relevant and an irrelevant part by means of a Kawasaki-Guntron projector $\mathcal{P}$ $\rho_{irr}(t) = \rho - \mathcal{P}\rho(t)$, where $\mathcal{P}\rho(t)$ is the relevant part and he ends up with a first order approximation which leads to an equation that can be interpreted as the quantum Boltzmann equation including the desired term $\mathbf{F} \cdot \mathbf{v}\partial/\partial\omega$; see Röpke [23].

At this point we emphasize that all variants of Boltzmann equations need classical or quantum mechanical equations for the microscopic dynamics. These equations are reversible in its nature. Since any type of Boltzmann equations is irreversible an additional technique is needed to randomize the dynamical equations. Boltzmann had already used a corresponding argument to derive his interaction term. A generalized form of Boltzmann's argument is known as Markovian limit. In his derivation of Mahan's quantum Boltzmann equation Prüstel cancelled the non-diagonal terms of the relevant observable and showed that it is equivalent with a Markovian limit where a decoherence time $\tau_{decoh} \sim 1/(kT)$ is introduced. Therefore decoherence is established by considering a certain subspace in the space of observables and consecutive cancelling of non-diagonal elements of the relevant observable. Decoherence aspects are discussed in the paper of Mathis *et al.* [22] where it is established by reducing the density matrix under consideration of a factor of the tensor

product describing the state space. For fully quantum transport processes in semiconductors the many-body Schrödinger equation has to be used that will be discussed in the following chapter.

## 1.2. Quantum Mechanical Transport

The ability of a semiconductor crystal to carry a macroscopic quantity like electric current is determined by the band diagram or the electronic spectrum of the crystal. The crystal lattice of a semiconductor is consisted of a large number of ionized atoms providing the electrons a very complex energy profile. For temperatures above $0K$ the lattice atoms move around (vibrate) their zero position causing a time dependent perturbation of the lattice structure. In a more detailed modelling, we have to include the fact that electrons interact with each other and with the lattice. In the Schrödinger picture of quantum mechanics, the equation of motion for electrons in a crystal is

$$-i\hbar\frac{\partial}{\partial t}\hat{\Psi}(\{\mathbf{r}_i, s_i\}\{\mathbf{R}_j\};t) = H(t)\hat{\Psi}(\{\mathbf{r}_i, s_i\}\{\mathbf{R}_j\};t). \tag{9}$$

Thereby $\mathbf{r}_i$ are the electronic and $\mathbf{R}_j$ the core coordinates.[1] $s_i$ denotes the spin coordinate. $\hat{\Psi}(\{\mathbf{r}_i, s_i\}\{\mathbf{R}_j\};t)$ is the complete wave function of the many-particle system and $H$ the Hamilton-operator for the particular system of interest. The indices $i$ and $j$ determine the number of electrons and ionized atoms respectively in the crystal.

### 1.2.1. *Time independent Schrödinger equation*

We assume that the cores are spatially fixed in the system and the configuration of lattice atoms is time invariant. This leads to two simplifications for Eq. (9): Firstly, the complete electron state $\hat{\Psi}$ is a function only of the electron and spin coordinates and time

$$\hat{\Psi} = \hat{\Psi}(\{\mathbf{r}_i, s_i\};t)$$

and secondly, Hamilton operator $H$ is time-independent. For a (perfect) semiconductor crystal, the Hamilton operator is given by

$$H = \sum_{i=1}^{N}\left[-\frac{\hbar^2}{2m}\nabla_i^2 + v_{\text{ext}}(\mathbf{r}_i)\right] + \sum_{i<j}^{N}\frac{q^2}{\|\mathbf{r}_i - \mathbf{r}_j\|}. \tag{10}$$

[1] $\{\mathbf{r}_i, s_i\}$ and $\{\mathbf{R}_j\}$ represent the set of all electronic and atomic coordinates, e.g. $\{f_i\} = (f_1, f_2, \ldots f_i \ldots f_N)$.

The first term on the right hand side denotes the kinetic energy of each electron, the second term, the periodic lattice potential, represents the interaction of the electrons with the atoms. The last term in Eq. (10) gives the interaction between the electrons in the crystal.

The electron state $\hat{\Psi}(\{\mathbf{r}_i, s_i\}; t)$ can be written as product of a pure time dependent and spatial part $\hat{\Psi}(\{\mathbf{r}_i, s_i\}; t) = \Phi(t)\Psi(\{\mathbf{r}_i, s_i\})$, and the time and spatial dependent parts can be separated. The time dependent part $\Phi(t)$ holds

$$i\hbar \frac{d}{dt}\Phi(t) = E\Phi(t), \quad \text{with} \quad \Phi(t) = e^{-i\frac{E}{\hbar}t}, \tag{11}$$

whereby the constant due to the integration is neglected. Substituting the solution for $\Phi(t)$ into (9) then gives for the spatial dependent part $\Psi(\{\mathbf{r}_i, s_i\})$

$$H\Psi(\{\mathbf{r}_i, s_i\}) = E\Psi(\{\mathbf{r}_i, s_i\}), \tag{12}$$

which is the stationary Schrödinger equation. Eq. (12) is a eigenvalue problem with appropriate boundary conditions. All solutions $\Psi(\{\mathbf{r}_i, s_i\})$ are functions of the Hilbert space $\mathscr{H}$.

### *1.2.2. Single electron approximation*

If we neglect the Fermi characteristic of electrons and use the Hartree approximation [24], the many-body problem is reduced to a formal single-particle problem. The electron-electron interaction is restricted to the Coulomb interaction. With the general definition of electron density

$$n(\mathbf{r}) = \sum_{i=1}^{N}\sum_{s} \psi_i^*(\mathbf{r}, s)\psi_i(\mathbf{r}, s) \tag{13}$$

we can rewrite the Coulomb interaction term and obtain

$$v_{\text{coul}}(\mathbf{r}) = \sum_{i=1}^{N} \int d^3r' \psi_i^*(\mathbf{r}') \frac{q^2}{\|\mathbf{r} - \mathbf{r}'\|} \psi_i(\mathbf{r}') = \int d^3r' \frac{q^2}{\|\mathbf{r} - \mathbf{r}'\|} n(\mathbf{r}'). \tag{14}$$

In conclusion one gets the classical potential energy for the direct interaction. The Hartree approximation can be described as a mean field theory, whereby a single electron is moving in potential due to presence of the other electrons, but is not interacting with them. The potential acting on the electrons is the same for every electron. The potential $v_{\text{coul}}(\mathbf{r}) = qU(\mathbf{r})$ itself can be calculated from the Poisson equation

$$\nabla \cdot (\epsilon(\mathbf{r})\nabla U(\mathbf{r})) = -qn(\mathbf{r}), \tag{15}$$

with $qn(\mathbf{r})$ as the charge density. The resulting single electron equation of motion in the Hartree approximation is given by[2]

$$\left[-\frac{\hbar^2}{2m}\nabla^2 + v_{\text{ext}}(\mathbf{r}) + v_{\text{coul}}(\mathbf{r})\right]\psi_m(\mathbf{r}) = \varepsilon_m\psi_m(\mathbf{r}). \tag{16}$$

The solution of the Poisson Eq. (15) and the equation of motion (16) has to be obtained self-consistently. Both equation are cross coupled due to the potential $v_{\text{coul}} = qU$ and the electron density $n$, see Eq. (13). Note that a single particle Schrödinger equation can only describe pure coherent transport of electrons throughout the device. For any loss of coherence due to inelastic scattering we need a generalized modelling concept.

### *1.2.3. Effective mass equation*

Due to the periodicity of the crystal lattice potential $v_{\text{ext}}$ we can separate the solution of the crystal Schrödinger equation into a periodic (Bloch functions) and a non-periodic part (envelope functions)

$$\psi(\mathbf{r}) = \hat{\psi}(\mathbf{r})u(\mathbf{r}), \tag{17}$$

and the equation of motion (16) is simplified to the effective mass equation

$$\left[-\frac{\hbar^2}{2m^*}\nabla^2 + v_{\text{coul}}(\mathbf{r})\right]\hat{\psi}_m(\mathbf{r}) = \varepsilon_m(\mathbf{k})\hat{\psi}_m(\mathbf{r}), \tag{18}$$

whereby the single electron orbital $\hat{\psi}_m(\mathbf{r})$ has to be distinguished from $\psi(\mathbf{r})_m$ in Eq. (16). Roughly speaking, we can say that the effective mass replaces the periodic potential of the crystal lattice but still contains structural properties of the crystal. The corresponding dispersion relation for Eq. (18) depends on the particle type (electrons or light or heavy holes etc.). For example, for electrons at the conduction band edge the dispersion relation is usually parabolically approximated

$$\varepsilon_m(\mathbf{k}) = E_{c0} + \frac{\hbar^2}{2m^*}(k_x^2 + k_y^2 + k_z^2), \tag{19}$$

whereby $\mathbf{k} = (k_x, k_y, k_z)$ is the wave vector and $E_{c0}$ the conduction band edge. All needed quantities characterizing transport processes, like electron density $n$ and current density $\mathbf{J}$, can be directly computed from the envelope function $\hat{\psi}(\mathbf{r})$ and it is not necessary to calculate the actual orbital $\psi(\mathbf{r})$, see e.g. [25].

[2]The spin coordinate $s_i$ can be neglected in the single electron picture, when no magnetic effects are considered.

### *1.2.4. Spatial dependent effective mass*

We assume a quasi-one dimensional solid, consisting of different materials (like a metal-oxide-semiconductor structure). The spatial coordinates are arranged so that the transport is happening in the $x$-direction and the $y, z$ plane is the transverse plane. The material is independent from the $y, z$ coordinates and changes only in the transport direction and the effective mass is a function of $x$, e.g. $m^* = m^*(x)$. The Hamilton operator from corresponding Schrödinger equation $H\hat{\psi} = E\hat{\psi}$ can be separated into a transverse part $H_T$ and a longitudinal part $H_L$

$$H \equiv H_T + H_L \quad \text{and} \quad \hat{\psi}(\mathbf{r}) = \psi(x) \cdot \varphi(y, z). \tag{20}$$

For a solid with a very large cross section area (effectively infinite cross section) any confining potential in the transverse direction can be neglected.[3] The solution for the transverse direction follows directly in terms of plane waves

$$\varphi(\mathbf{r}_\perp) = \frac{1}{\sqrt{S}} e^{i\mathbf{k}_\perp \cdot \mathbf{r}_\perp}. \tag{21}$$

$\mathbf{k}_\perp$ and $\mathbf{r}_\perp$ are both vectors in the $y - z$ plane. $S$ is the transverse cross sectional area.[4] The spatial dependence of $m^*(x)$ is accounted with the assumption

$$\frac{\hbar^2}{2} \frac{\partial}{\partial x} \frac{1}{m^*(x)} \frac{\partial}{\partial x} \tag{22}$$

which is in fact still a Hermitian operator and the eigenvalues remain real. The usage of spatial dependent mass operator (22) was controversial (see e.g. [26]) but accepted in nowadays [27] and commonly used in transport modeling [28, 29].

The Schrödinger equation for a spatial dependent mass $m^*(x)$ is given by

$$\left[ -\frac{\hbar^2}{2m^*(x)} \frac{\partial^2}{\partial \mathbf{r}_\perp^2} - \frac{\hbar^2}{2} \frac{\partial}{\partial x} \frac{1}{m^*(x)} \frac{\partial}{\partial x} + v_{\text{Coul}}(x) \right] \hat{\psi}(\mathbf{r}) = E\hat{\psi}(\mathbf{r}). \tag{23}$$

The spatial dependent effective mass Eq. (23) can be reduced to a one dimensional equation in transport direction

$$\left[ -\frac{\hbar^2}{2} \frac{\partial}{\partial x} \frac{1}{m^*(x)} \frac{\partial}{\partial x} + v_{\text{Coul}}(x) + E_c(x) \right] \psi(x) = \left( E - \frac{\hbar^2 k_\perp^2}{2m^*(x)} \right) \psi(x). \tag{24}$$

[3] Free electron problem in transverse direction.
[4] Note that $S$ cancels out, when we calculate any physical quantity like current density etc.

$E$ is the total energy and $\varepsilon_\perp$ the transverse eigenenergy

$$E = \varepsilon_x + \varepsilon_\perp, \quad \varepsilon_\perp = \frac{\hbar^2 k_\perp^2}{2m^*(x)}. \tag{25}$$

Due to the energy conservation law one can write equivalently for (25)

$$E = \varepsilon_x^L + \frac{\hbar^2 k_\perp^2}{2m_L^*} = \varepsilon_x + \frac{\hbar^2 k_\perp^2}{2m^*(x)}, \tag{26}$$

whereby $\varepsilon_x^L$ and $m_L^*$ are respectively the longitudinal eigenenergy and the (constant) effective mass at the point $x = 0$, which would be a lead[5] (or contact) when we consider a real device. Thus (24) changes to

$$\left[-\frac{\hbar^2}{2}\frac{\partial}{\partial x}\frac{1}{m^*(x)}\frac{\partial}{\partial x} + v_{\text{eff}}(\mathbf{k}_\perp, x)\right]\psi(x) = \varepsilon_x^L \psi(x) \tag{27}$$

with an effective potential dependent on direction $x$ and the transverse modes $\mathbf{k}_\perp$

$$v_{\text{eff}}(\mathbf{k}_\perp, x) = v_{\text{Coul}}(x) + E_c(x) + \frac{\hbar^2 k_\perp^2}{2m_L^*}\left(1 - \frac{m_L^*}{m^*(x)}\right). \tag{28}$$

The corresponding Poisson equation is given by

$$\frac{d}{dx}\epsilon(x)\frac{d}{dx}U(x) + q[N_d^+(x) - N_A^-(x) - n(U,x)] = 0, \tag{29}$$

with the densities of the acceptor $N_A^-(x)$ and donor ions $N_d^+(x)$, respectively, the electronic charge $q$ and a spatial dependent permittivity $\epsilon(x)$, caused by the device structure.

As a short summary, the two basic equations for coherent quantum transport are given by Eq. (27) and (29). The two equations have to be solved self-consistently, since they are cross-coupled due to

$$n(x) = \sum_\alpha \|\psi_\alpha(x)\|^2 f_0(\varepsilon_\alpha - \mu) \tag{30}$$

and $v_{\text{coul}}(x) = qU(x)$. $f_0$ is the Fermi function (see Eq. (47)) and $\mu$ the Fermi level.

## 1.3. Solving Transport Equations

A main difficulty in calculating the electron transports is to find an adequate method to solve the either semi-classical or the quantum mechanical transport

[5] Indicated by the superscript and index "L".

equation with the appropriate boundary conditions. As already emphasized, an electronic device has at least two contacts and is therefore an open system with open boundary conditions. The remaining part of this sections gives a short review about important approaches to solve transport equations. Due to the importance in the past, we start with semi-classical transport models.

### *1.3.1. Boltzmann equation and Wigner function approach*

The Boltzmann Eq. (4) gives us the balance-equation for the number of particles $N(t)$ being inside the volume element $d^3rd^3v$ of phase-space at the time $t$, see Eq. (1). They will be scattered into and out of this volume element and will be accelerated by external fields, e.g. the electric field **E**. In thermodynamical equilibrium we are able to get exact solutions from the Boltzmann equation. The Drift-Diffusion model (see Eq. (5)), the momentum-expansion of the Boltzmann equation, leads us to the continuity equation and an equation for the current-density $\mathbf{j} = \mu n \nabla E_F$ with the mobility $\mu$, the electron density $n$ and the Quasi-Fermi level $E_F$.

Taking into account quantum mechanical effect Wigner introduced a function analog to the classical probability density and containing the classical limit, the Wigner-function $f_W$ [9].

Let $\psi_n$ be the eigenfunctions and $\varepsilon_n$ the eigenenergies for our system, described by the Schrödinger Eq. (18). In the thermodynamical equilibrium the density-matrix is $\rho\left(\mathbf{r}, \mathbf{r}'\right) = \sum_n e^{\frac{E_n}{KT}} \psi_n\left(\mathbf{r}\right) \psi_n\left(\mathbf{r}'\right)$ and the Wigner-function can be expressed as the Fourier-transformed of this density-matrix in center-of-mass coordinates.

$$f_W\left(\mathbf{x}, \mathbf{p}\right) = \left(\frac{1}{\pi\hbar}\right)^3 \int e^{\frac{2i}{\hbar}\mathbf{p}\cdot\underline{y}} \rho\left(\mathbf{x}+\mathbf{y}, \mathbf{x}-\mathbf{y}\right) d^3y \tag{31}$$

Now, as Wigner showed, it is possible to gain information about a quantum system without solving Eq. (18), i.e. without determining the eigenstates or eigenvalues of our system.

Ancona was able to derive the Density-Gradient-method using the Wigner function approach, see e.g. [14, 30]. His result can be seen in a kind of generalized drift-diffusion equations with an additional correction-term, taking into account quantum-mechanical effects in the lowest degree. The Density-Gradient-method is most often used in simulations of semiconductor devices.

Finding the solution of the Boltzmann equation is a difficult problem since the distribution function has six arguments in the three dimensional case. The most widely technique for evaluating the Boltzmann equation is the Monte Carlo method [18]. Using this method the Boltzmann equation is not solved directly, but one rather simulates the motion of classical electrons subjected to a combination of free flight motion and instantaneous random scattering

events. The distribution function is then estimated by statistical averages over long times or many particles. The velocity and the position of each particle is integrated over the time between two collisions take place. Other random values determine the particular scattering mechanism and the velocity of the electron after the collision. After the collision takes place, the free-flight motion of the electron is again integrated until the next collision occurs. This procedure is performed for all electrons in the chosen ensemble to evaluate the time evolution of the device.

The Monte Carlo method permits to include other physical effects, such as detailed energy-band structure, electron-electron interaction and a more detailed description of scattering events.

### *1.3.2. 1-Particle-Schrödinger equation – nextnano³*

nextnano³ is a versatile simulation software tool mainly developed at the "Physik Department and Walter Schottky Insitut of TU München", see e.g. [31]. Besides the 3D simulation of pure quantum mechanical devices like quantum dots it is also capable to calculate one or higher dimensionally and fully quantum mechanically the transport in classical devices. nextnano³ contains a self-consistent Schrödinger Poisson solver, whereby self-consistency is achieved by introducing a spatial dependent quasi Fermi levels $E_F(\mathbf{r})$. The solutions of the Schrödinger Eq. (18) are assumed as a superposition of plane waves and the energies of these solutions are well defined by the dispersion relation $E(\mathbf{k})$. But, first of all the many-band-kp-Schrödinger equation is solved completely to get a good approximation for the band structure. This gives the density of charges ($n$ for electrons and $p$ for holes) by weighting the exact quantum mechanical states with the local Fermi levels. The local Fermi levels are obtained from the global current-conservation $\nabla \cdot \mathbf{j}_{n,p} = 0$, whereby $\mathbf{j}_n = \mu n \nabla E_{F,n}(\mathbf{r})$ for electrons and $\mathbf{j}_p = \mu p \nabla E_{F,p}(\mathbf{r})$ for holes.

For a summary the method is divided in two parts. In the first step the quasi-Fermi level is hold constant while the Schrödinger- and Poisson equation is solved self-consistently to get the new potential and the new quantized states. In the second step the potential and the states are fixed while determining the new Quasi-Fermi level with the current equation. This loop has to be repeated until self-consistency is reached.

### *1.3.3. Scattering-Matrix-Approach*

The scattering matrix represents the solution of the Schrödinger Eq. (18) for a sample that is connected to semi-infinite leads, see [32] or [33]. In this method, carrier transport is viewed as the transmission and reflection of carrier fluxes

within a semiconductor. The simulation domain is subdivided into thin slices (1D) or meshes (2D), so that these regions are sufficiently small to assume constant doping and fields within. Transport across each region is described by a matrix equation which relates the incident carrier fluxes to the emerging fluxes, through the transmission coefficient of a scattering matrix. The potential term in the Schrödinger Eq. (18) is augmented with an additional potential $V(\mathbf{r})$ representing any impurities. The boundary conditions are chosen in a way so that the wave function vanishes outside of the sample and the leads. In this scheme the solution of our problem is a combination of plane waves moving towards and from the sample.The wave functions are normalized such that they carry unit flux. Inside a sample the solution of the Schrödinger equation is described by incoming $\psi^i$, outgoing waves $\psi^o$ and evanescent waves, which are solutions with a complex wave vector. Far from the probe the evanescent mode will vanish. The scattering matrix can be divided into transmission and reflection matrices $r$, $r'$, $t$ and $t'$. For a wave approaching the sample through the left lead, the reflection matrix describes the reflected wave exiting through the left lead, and the transmission matrix t describes the transmitted wave in the right lead. Similarly, $r'$ and $t'$ describe reflection and transmission for waves coming from the right lead. Considering flux conservation demand the scattering matrix to be unitary.

For the case of serial scattering regions the description with transfer matrix can be used. This matrix relates the amplitudes in the left to the right of the sample. For the transfer matrices serial processes are expressed to be multiplicative. This multiplicative composition law points out the transfer matrix to be the ideal candidate for describing quantum transport through a disordered wire.

### *1.3.4. Pauli-Master-Equation*

The method of using the Pauli-Master-equation for our transport problem has been pointed out by Fishetti *et al.* [34]. The principal in a shortcut: first of all solve the Schrödinger- and Poisson equation with eigenfunction approach and then use the eigenfunction as a basis for the quantum Liouville-equation and derive the Pauli-master equation. The Pauli-master equation throws out directly the occupation of states. The transition rates can now be calculated with the help of Fermi's-golden-rule. Let us have a quick look at this formalism.

Let $\psi_\eta(\mathbf{r})$ be a basis of the one-particle Hilbert space, describing our device and $\psi^n(\mathbf{r}) = \sum_\mu a_\mu^n(t)\psi_\mu(\mathbf{r})$ the state of our N-body-system at $t = 0$ we can use the density-matrix $\rho_{\mu\nu} = \sum_{n=1}^N a_\mu^n(t)a_\nu^{n*}(t)$ to write the Liouville equation

$$\frac{\partial\rho}{\partial t} = \frac{i}{\hbar}\mathcal{L}\rho + \left(\frac{\partial\rho}{\partial t}\right)_{\text{reservoir}} - \frac{\rho - \rho^{eq}}{\tau_s}. \tag{32}$$

In this context $\left(\frac{\partial \rho}{\partial t}\right)_{\text{reservoir}}$ takes the exchange with the reservoir into account, the third term realizes the influence of scattering inside our device with the scattering-time $\tau_s$ and the density in equilibrium $\rho^{eq}$. Using the basis-states of $H_0$ we reach the Pauli-Master equation and find the diagonal elements of the density-matrix $\rho$.

To use the sketched scheme for our transport problem we first of all have to solve the Schrödinger equation for an initial potential using mixed boundary conditions. We get bound-, left- and right-propagating states. The next is the calculation of transition-probabilities and the population of the states according to the Pauli-master-equation. The effect of the contact regions in our semiconductor device is phenomenologically expressed by the term $\left(\frac{\partial \rho}{\partial t}\right)_{\text{reservoir}}$. Each contact is mapped with a quasi-fermi-level, which has to be fitted to ensure the charge neutrality and current conservation in this region while performing the self-consistent loop. Hereafter the Poisson equation should be solved etc. Note that the Pauli-Master-Equation approach covers in general both coherent and incoherent transport.

### *1.3.5. NEGF formalism*

A more sophisticated approach to quantum transport theory is supplied by the Green's function formulation of many-body theory. The non equilibrium Green's function (NEGF) theory was formulated by Kadanof and Baym in 1962 [35]. The application of non equilibrium Green's functions for the calculation of mesoscopic transport processes was mainly advanced by the group around S. Datta, R. Lake and M. Lundstrom [29, 36] and the NEGF is also the basis of quantum simulator `nemo`, see [37]. A very good introduction to the power of the NEGF formalism can be found in the two books [33] and [38] by S. Datta.

Roughly summarized, the non equilibrium Green's functions are defined by the expectation values of single-particle creation and annihilation operators. They describe the time evolution of the system. The Green's function is found by solving the Dyson equation, which is an integrated variant of the Schrödinger equation. The application of the NEGF to a MOS structure on the basis of the single electron Schrödinger equation will be shown in more detail in the next two sections. The presented example will exhibit stationary coherent transport, since this simplifications are appropriate for our aim, the analysis of tunneling currents in circuit simulations. However, the NEGF can be extended to include incoherent transport aspects as well as time dependent phenomena, see [35, 39, 40] and [33].

## 2. Self-consistent Transport Modeling

Modeling an electronic device as an open system means that we have to deal system of infinite extent. Thinking of a numerical calculation or simulation of such a system, means discretizing this infinite system and we would obtain matrices of infinite size, which would be intractable. The non-equilibrium Green's functions formalism (NEGF) offers a model for such open system, whereby the corresponding matrices are of finite extend (covering only the device region) and the coupling to the open environment is included in the finite discrete system. This section gives the most important conceptional steps of the NEGF and shows the calculation of coherent transport through multi-layered semiconductor structure. As we will see, the NEGF does not solve the Schrödinger equation directly but it calculates adequate quantities, including the needed electron density and the current density. The usage of a NEGF formalism to estimate tunneling currents might seem to much effort, in this case the Scattering matrix and the Transmission formalism would be sufficient. But our decision for the NEGF is explained by the versatility of this approach and the long term aim to extend considerations to incoherent and time dependent phenomena in charge transport.

Although all equations in the following have to be seen as discretized, e.g. differential equations change to matrix equations, we skip all considerations about discretization to the next section.

### 2.1. Green's Function for Coupled Device

For simplicity, we consider a system consisting of a device of finite dimension in $x$ direction and with very large extend in transverse $(y, z)$ direction and two semi-infinite electron reservoirs (contacts). The device is coupled to the two contacts, whereby the contacts are independent from each other. The Schrödinger equation for a isolated contact (i.e. contact 1) is given by

$$\left[\varepsilon_1 - H_1(x)\right]\psi_1(x) = 0. \tag{33}$$

We modify this equation to couple the isolated system with the environment and write

$$\left[(E + i\eta)\mathbf{1} - H_1(x)\right]\psi_1(x) = \mathscr{S}_1, \quad \eta \to 0, \tag{34}$$

whereby $E$ is the independent energy variable and not the eigenvalue of the system. The term $i\eta\psi_1$ can be read as the extraction of the electrons from the contact and $\mathscr{S}_1$ as the re-injection of electrons from externals sources [38]. The extraction and re-injection of electrons keep the systems in equilibrium with its surroundings and maintains a constant electro chemical potential, see [38]

for further details. It is important to note that Eq. (34) is not a Schrödinger equation, but still gives the dynamics of a coupled system.

For the coupled contact-device-contact structure we obtain an equation describing the dynamics of the coupled system

$$\begin{bmatrix} (E+i\eta)\mathbf{1}-H_1 & -\tau_1^+ & 0 \\ -\tau_1 & E\mathbf{1}-H_d & -\tau_2 \\ 0 & -\tau_2^+ & (E+i\eta)\mathbf{1}-H_2 \end{bmatrix} \times \begin{bmatrix} \psi_1+\chi_1 \\ \psi_d \\ \psi_2+\chi_2 \end{bmatrix} = \begin{bmatrix} \mathscr{S}_1 \\ 0 \\ \mathscr{S}_2 \end{bmatrix}, \tag{35}$$

whereby $\mathbf{1}$ is the appropriate unity operator to maintain mathematical correctness. The wave functions for the contacts are divided into an incident part $\psi_{1,2}$ (also corresponding to the waveform of the isolated contacts 1,2) and a reflected waveform $\chi_{1,2}$. With Eq. (35) and (34) we can write

$$\left[(E+i\eta)\mathbf{1}-H_1\right]\chi_1-\tau_1^+\psi_d=0. \tag{36}$$

And the reflected waveform $\chi_1$ in contact 1 can be estimated with

$$\chi_1=g_1\tau_1^+\psi_d, \tag{37}$$

i.e., the reflected waveform is a response due an excitation $\psi_d$ in the coupled device, whereby

$$g_1=\left[(E+i\eta)\mathbf{1}-H_1\right]^{-1} \tag{38}$$

is the resolvent for the isolated contact. A corresponding expression can also be derived for contact 2

$$\chi_2=g_2\tau_2^+\psi_d, \quad g_2=\left[(E+i\eta)\mathbf{1}-H_2\right]^{-1}. \tag{39}$$

To described transport processes in the device, we need to estimate the Green's function $G_d$ for the coupled device. From Eq. (35) follows

$$\left[E\mathbf{1}-H_d\right]\psi_d-\tau_1\chi_1-\tau_2\chi_2=\tau_1\psi_1+\tau_2\psi_2. \tag{40}$$

With Eq. (37) $\chi_{1,2}$ can be substituted, which gives

$$\left[E\mathbf{1}-H_d-\Sigma_1-\Sigma_2\right]\psi_d=S. \tag{41}$$

Hence, the Green's function $G_d$ for the coupled device is given by

$$G_d=[E\mathbf{1}-H_d-\Sigma_1-\Sigma_2]^{-1}. \tag{42}$$

and the wave function of the device is given by

$$\psi_d=G_dS. \tag{43}$$

The additional terms $\tau_1^+ g_1 \tau_1$ and $\tau_2^+ g_2 \tau_2$ incorporate the coupling of the finite device to the semi-infinite contacts. Both terms are called self-energies, defined by

$$\Sigma_1 \equiv \tau_1 g_1 \tau_1^+, \quad \Sigma_2 \equiv \tau_2 g_2 \tau_2^+. \tag{44}$$

For semi-infinite contacts, regular shaped and with well-defined transverse modes, the self-energies can be calculated analytically [33]. The source term $S$ with a similarly meaning like $\mathscr{S}_{1,2}$ is defined by

$$S = S_1 + S_2, \quad S_{1,2} = \tau_{1,2} \psi_{1,2}. \tag{45}$$

## 2.2. Electron Density

In the semi-classical approach the electron density in equilibrium is given by

$$n = \int_{E_c}^{\infty} N(E) f(E) dE, \tag{46}$$

see e.g. [41] or [42]. $N(E)$ is the density of states, i.e., $N(E)dE$ gives the number of states in the interval $[E, E + dE]$. $f(E)$ denotes the statistical distribution function, which is in case of electrons the Fermi-Dirac distribution function,[6] since electrons are fermions. The Fermi function is defined as

$$f_0(E, \mu) = \frac{1}{1 + e^{\frac{E-\mu}{kT}}}, \tag{47}$$

whereby $\mu$ is the Fermi energy, which is usually obtained from the charge neutrality condition [42].

In the NEGF formalism the density of states can be obtained from the spectral function $A(E)$, which is defined by

$$A(E) \equiv i\big(G(E) - G^+(E)\big), \tag{48}$$

and can be seen as a more generalized concept of the density of states. The density of states is given by

$$N(E) = \sum_{\alpha} \delta(E - \varepsilon_\alpha), \tag{49}$$

and we can write for $A(E)$

$$A(x, x'; E) = \sum_{\alpha} \psi_\alpha(x) \delta(E - \varepsilon_\alpha) \psi_\alpha^*(x'). \tag{50}$$

[6] or usually shortened as the Fermi function.

$G(E)$ in Eq. (48) is the Green's function of the system.[7] The spectral function for the coupled device is given with Eq. (48) by

$$A_d = i\left(G_d - G_d^+\right) = i\left(\frac{1}{E - H_d - \Sigma} - \frac{1}{E - H_d - \Sigma^+}\right), \tag{51}$$

which is identical to Eq. (50), when $\psi_\alpha$ corresponds to the state of the coupled device $\psi_{d,\alpha}$. Similarly to the "generalized" density of states $A(E)$ the density matrix $\rho$ as "generalized" electron density is introduced [33, 38]. To simplify the derivation of $\rho$, we reduce the problem and consider only the electron density in the device, which is caused by incident waves from contact 1. The density matrix of the device $\rho_d$ is then given by

$$\rho_d(x, x') = \sum_\alpha \psi_{d,\alpha}(x) f_0(\varepsilon_\alpha - \mu_1)\psi^*_{d,\alpha}(x'), \tag{52}$$

whereby are the eigenstates of the isolated contact 1. Using the definition of $A(E)$ in Eq. (48) and the fact that $\psi_d = G_d S_1$ we obtain

$$\begin{aligned}
\rho_d &= \int f_0(E - \mu) \sum_\alpha \psi_{1,\alpha}\delta(E - \varepsilon_\alpha)\psi^* 1, \alpha dE \\
&= \int f_0(E - \mu) G_d \tau_1 \left[\sum_\alpha \psi_{1,\alpha}\delta(E - \varepsilon_\alpha)\psi^*_{1,\alpha}\right] \tau_1^+ G_d^+ dE \\
&= \frac{1}{2\pi} \int f_0(E - \mu) G_d \tau_1 a_1 \tau_1^+ G_d^+ dE.
\end{aligned} \tag{53}$$

with $a_1 = i[g_1 - g_1^+]$ the spectral function of the (isolated) contact 1. As discussed earlier, the coupling between contact and device is incorporated with the selfenergies $\Sigma_{1,2}$. Using this concept, broadening functions $\Gamma_{1,2}$ can be defined [38]

$$\Gamma_{1,2} \equiv i\left[\Sigma_{1,2} - \Sigma_{1,2}^+\right], \quad \text{and} \quad \Gamma_{1,2} = \tau_{1,2} a_{1,2} \tau_{1,2}^+. \tag{54}$$

The density matrix changes to

$$\rho_d(x, x') = \frac{1}{2\pi} \int_{E=-\infty}^{\infty} f(E, \mu_1) A_1 \, dE \tag{55}$$

with

$$A_1 \equiv G_d \Gamma_1 G_d^+, \tag{56}$$

[7] In case of our coupled device $G(E)$ would comply $G_d(E)$ from Eq. (42). $G^+(E)$ is the Hermitian conjugate of $G(E)$ and corresponds to the advanced Green's function of the system, while $G(E)$ is the retarded Green's function.

see [33] and [43]. The density matrix for the complete coupled system is simply the sum over all contacts [44]

$$\rho_d(x, x') = \int_{E=-\infty}^{\infty} \Big( f(E, \mu_1) A_1 + f(E, \mu_2) A_2 \Big) \, dE. \tag{57}$$

The electron density $n(x)$ is the diagonal of the density matrix

$$n(x) = \frac{1}{\Omega} \rho(x, x')|_{x=x'}, \tag{58}$$

whereby $\Omega$ is the volume of the unit cell.

## 2.3. Current Density

According to the continuity equation, the electrical current is given by

$$I = -q \frac{\partial n}{\partial t}. \tag{59}$$

The probability current therefore holds

$$I_p \equiv \frac{\partial}{\partial t} \big( \sum_{\alpha} |\psi_d(x)|^2 \big). \tag{60}$$

The trace operation is identical with taking the summing over all $\alpha$ and we can write

$$\sum_{\alpha} |\psi_{d,\alpha}(x)|^2 = \sum_{\alpha} \psi^*_{d,\alpha} \psi_{d,\alpha} = \mathrm{Tr} \left[ \psi_d^+ \psi_d \right], \tag{61}$$

and obtain (see [38])

$$I_p = \frac{\partial}{\partial t} \big( \mathrm{Tr} \left[ \psi_d^+ \psi_d \right] \big). \tag{62}$$

The total (probability) current is zero, since we consider a non-equilibrium situation, caused by differing chemical potentials in the coupled reservoirs, but the situation is steady state. This means, all current going into the device, caused by contact 1 trying to bring the device in equilibrium with reservoir 1, is going out at contact 2, tyring to establish equilibrium with reservoir 2. Hence $I_1 = I_2 \equiv I$ and for the derivation of the current relation we only need to consider the current $I_1$ between contact 1 and device. The corresponding time dependent equation for the coupled system is given by

$$i\hbar \frac{\partial}{\partial t} \begin{bmatrix} \psi_1 + \chi_1 \\ \psi_d \end{bmatrix} = \begin{bmatrix} H_1 - i\eta & \tau_1^+ \\ \tau_1 & H_d \end{bmatrix} \begin{bmatrix} \psi_1 + \chi_1 \\ \psi_d \end{bmatrix}. \tag{63}$$

From Eq. (63) follows for the current $I_1$

$$I_1 = \frac{1}{i\hbar}\,\mathrm{Tr}\left[\psi_d^+\tau_1(\psi_1 + \chi_1) + (\psi_1^+ + \chi_1^+)\tau_1^+\psi_d^+\right], \tag{64}$$

which can be divided into two parts. One corresponding to the incoming component, connected with the incident wave function $\psi_1$. The second part is the outgoing component, corresponding to the reflected wave function $\chi_1$. Hence, we can write

$$I_1 = \underbrace{\frac{1}{i\hbar}\,\mathrm{Tr}\left[\psi_d^+\tau_1\psi_1 + \psi_1^+\tau_1^+\psi_d^+\right]}_{\text{inflow}} - \underbrace{\frac{1}{i\hbar}\,\mathrm{Tr}\left[\chi_1^+\tau_1^+\psi_d + \psi_d^+\tau_1\chi_1^+\right]}_{\text{outflow}}. \tag{65}$$

With the substitution $\psi_d = G_d S$, whereby $S = S_1 + S_2$, the inflow component of the current can be formulated as

$$I_{1,\mathrm{in}} = \frac{1}{i\hbar}\,\mathrm{Tr}\left[S^+G_d^+S_1 - S_1^+G_dS\right] = \frac{1}{i\hbar}\,\mathrm{Tr}\left[S_1S_1^+G_d^+ - S_1S_1^+G_d\right], \tag{66}$$

whereby we used $S_1^+S_2 = S_2^+S_1 = 0$. The definition of the spectral function was given in Eq. (48), and the inflowing current in contact 1 reduces to

$$I_{1,\mathrm{in}} = \frac{1}{\hbar}\,\mathrm{Tr}\left[S_1S_1^+A_d\right]. \tag{67}$$

For the isolated contact 1 we can write according to Eq. (55)

$$\rho_1(x,x') = \psi_1\psi_1^+ = \int \frac{f_1(E)}{2\pi}a_1(E)dE. \tag{68}$$

Since $S_1S_1^+ = \tau_1\psi_1\psi_1^+\tau_1^+$ we obtain the expression

$$S_1S_1^+ = \int \frac{f_1(E)}{2\pi}\tau_1a_1(E)\tau_1^+dE = \int \frac{f_1(E)}{2\pi}\Gamma_1dE. \tag{69}$$

The inflow current is then given by

$$I_{1,\mathrm{in}} = \frac{1}{2\pi\hbar}\int f_1(E)\,\mathrm{Tr}\left[\Gamma_1A_d\right]. \tag{70}$$

The outflowing component can be derived similarly like the inflow. We substitute the reflected wave functions $\chi_1 = g_1\tau_1^+\psi_d$ and $\chi_1^+ = \psi_d^+\tau_1g_1^+$, and write

$$I_{1,\mathrm{out}} = \frac{1}{i\hbar}\,\mathrm{Tr}\left[\chi_1^+\tau_1\psi_d + \psi_d^+\tau_1^+\chi_1^+\right] = \frac{1}{i\hbar}\,\mathrm{Tr}\left[\psi_d\psi_d^+\Gamma_1\right]. \tag{71}$$

For $\psi_d\psi_d^+$ we can write

$$\psi_d\psi_d^+ = \rho_d = \int \frac{1}{2\pi}G^n dE, \tag{72}$$

whereby $G^n = f_1(E)A_1 + f_2(E)A_2$ is the electron correlation function, see Eq. (57). Therefore, the outflow component is written with

$$I_{1,\text{out}} = \frac{1}{2\pi\hbar}\int \text{Tr}\left[\Gamma_1 G^n\right] dE. \tag{73}$$

The total (electrical) current $I$ is given with

$$I_1 = -2\frac{q}{h}\int (f_1 - f_2)\,\text{Tr}\left[\Gamma_1 G_d \Gamma_2 G_d^+\right] dE. \tag{74}$$

For further details see [38].

## 3. Numerical Transport Simulation

For an illustration of the numerical implementation of the NEGF formalism we consider a device structure consisting of two n-type silicon areas sandwiching an insulating oxide layer. The Si-oxide-Si device is connected on both sides to a contact. The complete device is pictured in Figure 1. In non-equilibrium, meaning the device is biased and the two Fermi levels $\mu_{1,2}$ of the left and right side reservoirs differ, a current flows through the structure and the insulating oxide layer. The considered situation is comparable to edge-direct-tunneling currents in modern MOSFET devices.

The following section starts with a discussion about the discretization of equation of motion and the calculation of all quantities of the NEGF formalism. Subsequent to the computation, we discuss the numerical solution of the Poisson equation, which we left out so far.

### 3.1. Method of Finite Differences

The calculation of physical quantities like currents and electron densities in devices is usually done with numerical simulations. This means, one has to

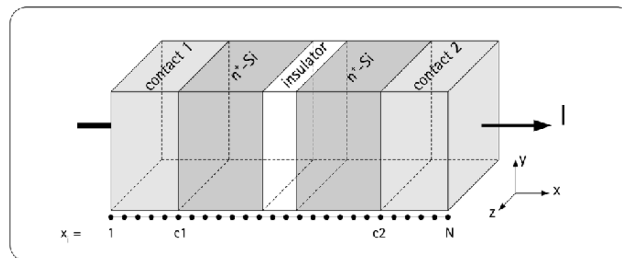


*Figure 1.* Si-oxide-Si device structure.

find a suitable discretization scheme for the underlying differential equations. In general, the equation of motion in the NEGF formalism and the coupled Poisson equation are discretized using the method of finite differences [29, 43, 45]. However, there also alternative discretization schemes to find in recent literature like the application of the finite element method in [46].

The 1-dimensional equation of motion for Si-oxide-Si structure with transport in $x$-direction (see Figure 1) is given by Eq. (27) on page 218. The finite difference form for (27) is written with

$$-t_{i-1,i}\psi_{i-1} + H_{d,i}\psi_i - t_{i,i+1}\psi_{i+1} = \varepsilon\psi_i, \tag{75}$$

with

$$H_{d,i} = \left[\frac{\hbar^2}{2s^2}\left(\frac{1}{m^-} + \frac{1}{m^+}\right) + E_{c,i} + v_{\mathrm{coul},i} + \varepsilon_\perp\left(\frac{m_L^*}{m_i^*} - 1\right)\right]. \tag{76}$$

The notation $f_i$ should be read as $f_i = f(x_i)$, whereby $x_i$ is the $i$-th discrete spatial point. The lattice spacing $s$, e.g. the distance between two discrete points, is equidistant. Furthermore we have

$$m^- = \frac{m_{i-1} + m_i}{2}, \quad m^+ = \frac{m_i + m_{i+1}}{2} \quad \text{and} \quad t_{i,j} = \frac{\hbar^2}{(m_i + m_j)s^2}. \tag{77}$$

Hence the differential Eq. (27) changes to a matrix equation. As one can see in Eq. (75), an arbitrary lattice point $i$ is coupled only to it's nearest neighbors with $t_{i,j}$, thus the finite difference approximation is a tight-binding model [29, 38]. Let us take look at the dispersion relation for the discretized device. In the contact region of the example (see Figure 1) the effective mass $m_{x_i}$ with[8] $i = 1, 2 \ldots c1, c2 \ldots N$ is constant and equals $m_L^*$, obviously. The discretized equations of motion in this part of the device can be simplified to a equation with a constant effective mass, see (18) and the discrete dispersion relation is given with

$$\varepsilon = v_{\mathrm{coul},i} + E_{c,i} + 2t(1 - \cos(ks)). \tag{78}$$

For very small $k \cdot s$, meaning the transition from the discrete to continuous case, the dispersion relation reduces to the parabolic band approximation. The open boundary conditions for the device are incorporated with the selfenergies, as stated in the previous section. For an 1-dimensional device, the derivation can be obtained following simply arguments as presented by Datta in [43]. From the matrix representation (75) we found that any lattice point couples only with its two direct neighbours (in the 1-dimensional case). This means that only the first point an the $N$-th point have to be "coupled" with the selfenergies to the

[8]Therefore, $i = c_1 + 1 \ldots c_2 - 1$ determines the Si-oxide-Si part of the device displayed in Figure 1.

reservoirs (semi-infinite contacts) on both sides. Hence, the selfenergies $\Sigma_{1,2}$ are matrices completely filled with zeros except one point:

$$\Sigma_1(1,1) = -\tilde{t}e^{jk_1 s}, \quad \Sigma_2(N,N) = \tilde{t}e^{jk_N s}. \tag{79}$$

The needed wave vectors $k_1$, $k_N$ can be estimated from the dispersion relation in Eq. (78).

With the above stated equations we are able to calculate all necessary quantities for the NEGF formalism, the discrete Green's function $G_d$ for the device

$$G_d(E,k_\perp) = \left[E\mathbf{1} - H_d - \Sigma_1 - \Sigma_2\right]^{-1}, \tag{80}$$

the spectral functions

$$A_{1,2}(E,k_\perp) = G_d(E,k_\perp)\Gamma_{1,2}(E)G_d^+(E,k_\perp), \tag{81}$$

and the broadening functions

$$\Gamma_{1,2}(E) = i\Big(\Sigma_{1,2}(E) - \Sigma_{1,2}^+(E)\Big). \tag{82}$$

The density matrix follows as an integral over the interested energy interval and the sum over all transversal $\mathbf{k}_\perp$-states

$$\rho = \frac{1}{2\pi}\sum_{k_\perp}\int_{E=-\infty}^{\infty}\Big[f_0(E,\varepsilon_{k_\perp},\mu_1)A_1(k_\perp,E) \\ + f_0(E,\varepsilon_{k_\perp},\mu_2)A_2(k_\perp,E)\Big]dE \tag{83}$$

with the Fermi functions given in (47) and the transversal eigenstates from Eq. (26). We can rewrite all equations to be explicit dependent on the transversal wave vector $\mathbf{k}_\perp$ instead of the transversal eigenstate $\varepsilon_\perp$. Using the periodic boundary conditions, the summation over all transverse wave vectors changes to an integral

$$\sum_{\mathbf{k}_\perp} \rightarrow \int d^2\mathbf{k}_\perp \frac{S}{4\pi^2} = \frac{S}{4\pi^2}\int 2\pi k_\perp dk_\perp, \tag{84}$$

whereby $S$ denotes the size of the transversal area. But it cancels out, when we calculate a real physical quantity like the electron density $n$. As we know from Eq. (58), the electron density at the discrete lattice point are the diagonal elements of the density matrix weighted by the volume $\Omega = S \cdot s$ of the discretized cell, see Eq. (58). Introducing a slightly changed density matrix $\rho'$

$$\rho' = \frac{1}{4\pi}\iint\Big[f_0(E,k_\perp,\mu_1)A_1(k_\perp,E) + f_0(E,k_\perp,\mu_2)A_2(k_\perp,E)\Big] \\ \times dEk_\perp dk_\perp, \tag{85}$$

the electron density can be calculated with

$$n(x_i) = \frac{1}{s}\rho'(x_i,x_i')|_{x=x_i} \tag{86}$$

without the knowledge of $S$.

### 3.2. Solution of The Poisson Equation

The Poisson equation of the example device in Figure 1 is discretized on the same spatial lattice as the equation of motion and we can write

$$\frac{1}{s^2}\left(\epsilon_i^- U_{i-1} - (\epsilon_i^- + \epsilon_i^+)U_i + \epsilon_i^+ U_{i+1}\right) + q\left[N_{D_i}^+ - N_{A_i}^- - n_i\right] = 0 \quad (87)$$

with

$$\epsilon_i^- = \frac{\epsilon_{i-1} + \epsilon_i}{2}; \quad \epsilon_i^+ = \frac{\epsilon_{i+1} + \epsilon_i}{2}. \quad (88)$$

For the solution of the Poisson equation we use a the standard Newton-Raphson algorithm (see e.g. [47]). Eq. (87) is rewritten as a matrix equation. The boundary conditions follow directly from the applied bias over the structure. When $V$ is the external voltage, the values of the first and the $N$-th point of the lattice are given by

$$\frac{1}{s^2 q}\left(\epsilon_1^- 0 - (\epsilon_1^- + \epsilon_1^+)U_1 + \epsilon_1^+ U_2\right) + \left[N_{D_1}^+ - N_{A_1}^- - n_1\right] = 0$$

$$\frac{1}{s^2 q}\left(\epsilon_N^- U_{N-1} - (\epsilon_N^- + \epsilon_N^+)U_N + \epsilon_N^+ V\right) + \left[N_{D_N}^+ - N_{A_N}^- - n_N\right] = 0.$$

Hence, the values at the boundary are fixed due to the applied voltage $V$. The solution of the Poisson equation is formulated as a problem of finding the roots of a discrete function $F$. For the $i$-th spatial point $F_i$ is given by

$$F_i = \frac{1}{qs^2}\left(\epsilon_i^- U_{i-1} - (\epsilon_i^- + \epsilon_i^+)U_i + \epsilon_i^+ U_{i+1}\right) + N_{D_i}^+ - N_{A_i}^- - n_i \quad (89)$$

and we have to solve

$$\sum_j \frac{\partial F_i^m}{\partial U_j^m}\delta U_j^{m+1} = \mathscr{J}_f(F_i^m)\delta U_j^{m+1} = -F_i^m, \quad j = 1, 2 \ldots N, \quad (90)$$

whereby $m$ denotes the iteration index and the sum of the Jacobian $\mathscr{J}_f$ on the left hand side runs over all $N$ points of the discrete lattice. The corrected value of $U$ is determined by

$$U^{m+1} = U^m + \delta U_j^{m+1}, \quad (91)$$

with $\delta U_j^{m+1}$ given by

$$\delta U_j^{m+1} = -\mathscr{J}_f^{-1}(F_m)F_m, \quad (92)$$

according Eq. (90). To calculate the derivation $\partial n/\partial U$ for the Jacobian $\mathscr{J}_f$ we use the approximation given in [29]

$$\frac{\partial n}{\partial U} \approx q\frac{\partial n}{\partial E_f}. \quad (93)$$

With Eq. (85) and (86) we obtain

$$\frac{\partial n}{\partial E_f} \approx \frac{2q}{s} \int \frac{dE}{2\pi} \int \frac{d^2\mathbf{k}}{4\pi^2} \left[ -\frac{\partial f_0(E, \mu_1)}{\partial E} A_1(k_\perp, E) - \frac{\partial f_0(E, \mu_2)}{\partial E} A_2(k_\perp, E) \right], \tag{94}$$

using the fact that the quasi Fermi level in contacts correspond to the chemical potentials $\mu_{1,2}$ in the coupled reservoirs 1 and 2, see [29]. The derivation of the Fermi function with respect to the Fermi level is given by

$$\frac{\partial f_{1,2}}{\partial E_f} = \frac{1}{kT} f_{1,2}(1 - f_{1,2}). \tag{95}$$

## 3.3. Numerical Solution

After reaching convergence in the self-consistent solution of the equation of motion and the Poisson equation, the current density is calculated with Eq. (74). The complete coupled and self-consistent solution of the equation for the dynamics (the Schrödinger equation) and for the electro-statics (the Poisson equation) follows the flow chart given in Figure 2. The flowchart shows the calculation for a certain external bias $V$. For a complete $J - V$ characteristic of a device, the depicted procedure has to be repeated for every bias value $V_n$. The calculation of a $J - V$ device characteristic usually starts at equilibrium

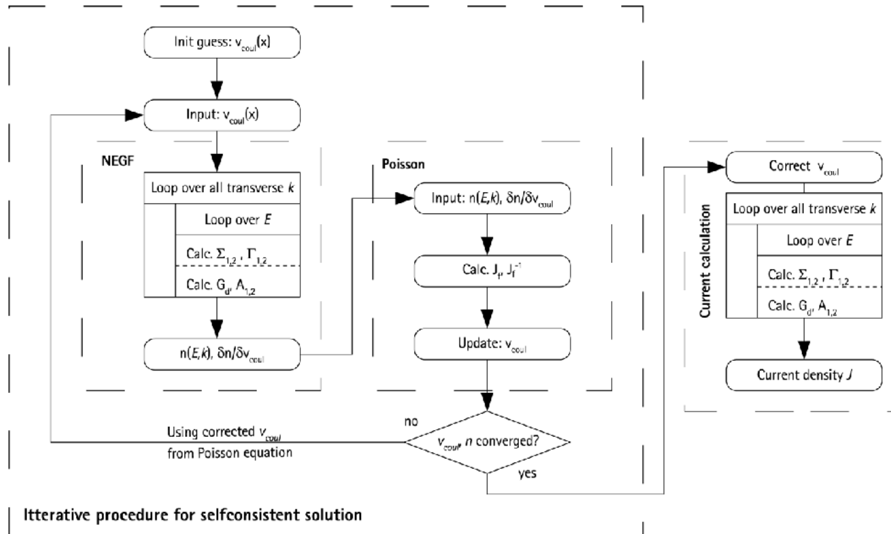


*Figure 2.* Flowchart of the iterative self-consistent solution for a certain external bias.

with $V = 0$, where a initial guess for $U$ is easily done. For the calculation for different bias points, a reasonable initial guess for $U$ is the converged $U$ of preceding bias point, assuming that the difference between the bias points is not too big.

## 4. Circuit Simulation and Applications

We started our analysis of the impact of quantum effects to circuit functionality with the most obvious effect: the gate direct tunneling currents. The very first studies about the influence of tunneling currents can be found in the publications from Dutton, Choi *et al.* [48–50]. We use this publications as references for our overall methodology.

In modern MOSFETs two different direct gate tunneling mechanisms have to be accounted: (1) the direct tunneling between the inverted channel and the gate, and (2) the tunneling between overlapping source/drain extensions and the gate (edge-direct-tunneling). To include quantum parasitics in circuit simulations we represent them as additional Q-sources.[9] This means that in case of the direct tunneling currents in MOS-devices, such as FETs and capacitors, we are using additional voltage controlled current sources together with common device models. The current sources are implemented as look-up-table models, which is the easiest way to represent the current-voltage pairs from the numerical quantum transport simulations. Between two different pairs the values are obtained with linear interpolation, done by SPICE.

Our Q-sources are placed comparable to the tunneling leakage model implemented in BSIM4 (see [51]). The tunneling model in BSIM4 model differs significantly in estimating the magnitude of the tunneling currents. In comparison to our approach, the BSIM4 tunneling model needs a lot of non physical fitting parameters (see [51]), but which adjust the BSIM4 model to measurements of real physical devices. The withdraw of this very high-level or in other words non-physical description is that it covers the magnitude of macroscopic quantities (e.g. current density) for a particular device due to fitting. It is limited when the general behaviour is needed and when the dimension shrinks further and the quantum mechanical behaviour of the charge carriers causes more than additional currents.

### 4.1. SRAM Cell

In the recent literature, see e.g. [1, 52], the exponential increase of gate tunneling current at decreasing oxide thickness is a growing concern to ULSI

[9] Q $\hat{=}$ quantum parasitic.

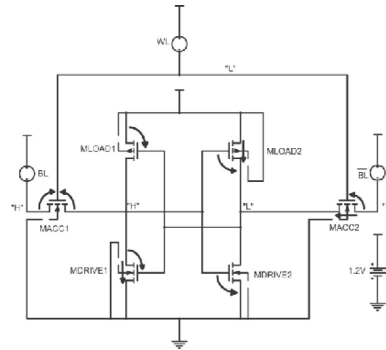


*Figure 3.* 6 transistor SRAM cell.

circuit performance and stability. But a direct influence of the quantum effects to the circuit functionality of static CMOS logic circuit itself is not expected to be a major problem [5]. In those cases only the strongly increasing off-state power dissipation is the main consequence [1]. As an example we simulated a 6-transistor SRAM cell [53] including our Q-sources. It showed that the ratio between the standard (or classical) leakage mechanisms and the direct tunneling leakage currents is reversing when the gate oxides gets thinner than 3 nm. The SRAM cell is depicted in Figure 3, whereby curved arrows show the tunneling currents and the straight arrows the conventional leakage currents. For a 2 nm oxide thickness flows total current of 9.2 pA caused by tunneling and the conventional leakage contributes only 2.9 pA to the power consumption. The simulation was made for the steady state situation depicted in Figure 3.

## 4.2. Domino-AND-2 Gate

In contrast to the "robustness" of static logic, dynamic logic and analog circuit functionality can be a critical case when the magnitude of tunneling current raises. It can be shown for a Domino-AND-2 gate that the circuit produces logical errors when the oxide thickness decreases beyond 2 nm [5]. The critical element in the Domino AND gate (see Figure 4) is the transistor $M_2$ at the input "A". In the precharge phase of the circuit (i.e. clock is "low", transistor $M_1$ is open) the capacitor $C_1$ is charged to $V_{dd}$ level, so that the inverter at the output produces the correct "low" level (the corresponding input signal pattern is depicted in Figure 5). In the evaluation phase (clock signal is "high") the transistor $M_1$ is switched off and $C_1$ remains on $V_{dd}$ as long the inputs "A" and "B" are zero. If we include the tunneling currents in the circuit simulation, we have an edge-direct tunneling in transistor $M_2$, which discharges $C_1$ as long the level on input "A" is "low". When the oxide thickness is under a critical value,

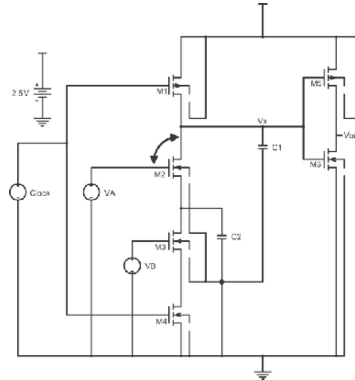

*Figure 4.* Domino AND 2 Gate.

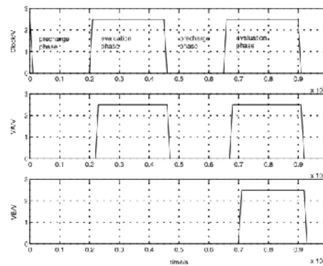

*Figure 5.* Input signals for Domino AND 2 Gate.

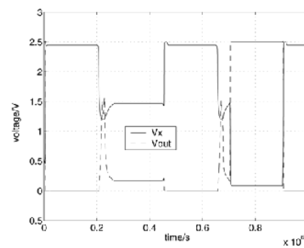

*Figure 6.* Output signals for Domino AND 2 Gate.

capacitor $C_1$ is discharged so quickly that $V_x$ falls bellow $V_{dd}/2$ even before $V_A$ on input "A" switches to a "high" level. In consequence, the inverter at the output produces a glitch with a magnitude higher than $V_{dd}/2$ (Figure 6), which has to be treated as a logical error – i.e. failure of the circuit functionality. A similar situation occurs when input "B" changes from "low" to "high" after a level change at input "A", see Figure 6.

## 4.3. Sample&Hold Circuit

The influence of gate direct tunneling currents in analog circuits can be shown with the example of a Sample & Hold circuit (suggested in [5]). The Spice schematic for a S&H circuit with a MOS capacitor as hold capacitance is shown in Figure 7. The switching transistors of the transmission gate and the MOS capacitor have a 2 nm oxide layer. In the transistor on-state the output waveform is directly following the input and the capacitance $C_1$ (see the Spice schematic in Figure 7) is charged to the current voltage level. With the charged MOS capacitor $M_3$ the output should remain on the last magnitude of the input when the transmission gate is switched off. But due to 2 nm insulating oxide, a direct tunneling current between the overlapping area of drain and gate and a direct tunneling in $M_3$ is discharging the output capacitance indicated be the arrows in Figure 7; and the output signal level is falling (see the dashed line in Figure 8) and does not remain as it should – circuit failure caused by Q-interference.

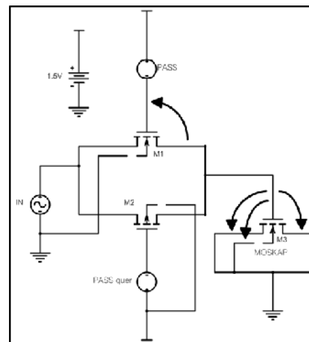


*Figure 7.* Sample & Hold circuit.

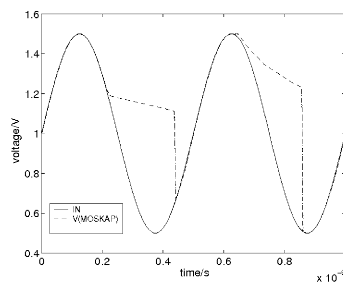


*Figure 8.* Input and output signals of a Sample & Hold circuit influenced by direct tunneling currents.

## 5. Conclusions

In this chapter, we tried to achieve two objectives: (1) to show that in future CMOS circuits, when length scale is in the domain around 20 nm and below, the charge carrier transport will be dominated by coherent transport and the drift-diffusion based device models will be too restricted and (2) to demonstrate that the functionality of classical circuits concepts can be substantially affected by parasitic quantum effects.

We showed a self-consistent NEGF-Schrödinger Poisson solver in detail, which allows the quantum mechanical calculation of coherent charge transport in semiconductors. Taking the results of the transport simulation we included parasitic quantum effects in high-level circuit simulators. Starting with the phenomena of direct tunneling currents in MOS circuits, we discussed different circuit examples, which all were affected in their functionality due to tunneling.

We believe among others [54] that the set of Schrödinger and Poisson equation will replace the various Drift-Diffusion models and hydrodynamic equations for device simulators in the <20 nm regime. Much work has to be done in order to maintain functionality of the important CMOS circuit concepts. More, former negligible quantum effects will disturb circuit functionality and the analysis of the influence of the tunneling currents can only be seen as a first step.

## 6. Acknowledgments

The Authors would like to thank Simon Fabel and Jan Bremer for their efforts to realise the numerical simulations.

## References

[1] Roy, K.; Mukhopadhay, S.; Mahmoodi-Meimand, H. "Leakage current mechanisms and leakage reduction techniques in deep-submicrometer CMOS circuits", *Proc. IEEE*, **2003**, *91(2)*, 305–327.

[2] Yang, N.; Kirlen Henson, W.; Wortman, J.J. "A comparative study of gate direct tunneling and drain leakage currents in N-MOSFETs with sub-2-nm gate oxides", *IEEE Trans. Electron Dev.*, **2000**, *47(8)*, 1636–1644.

[3] Yu, Z.; Dutton, R.W.; Kiehl, R.A. "Circuit/device modeling at the quantum level", *IEEE Trans. Electron Dev.*, **2000**, *47(10)*, 1819–1825.

[4] Vasileska, D.; Knezevic, I.; Akis, R.; Ahmed, S.; Ferry, D.K. "The role of quantization effects on the operation of 50 nm MOSFETs, 250 nm FIBMOS devices and narrow-width SOI device structures", *J. Comput. Electron.*, **2002**, *1*, 453–465.

[5] Choi, C.-H.; Nam, K.-Y.; Yu, Z.; Dutton, R.W. "Impact of gate direct tunneling current on circuit performance: A simulation study", *IEEE Trans. Electron Dev.*, **2001**, *48(12)*, 2823–2829.

[6] Huang, K. *Statistical Mechanics*, John Wiley & Sons, **1963**.
[7] van Roosbroeck, W.V. "Theory of flow of electrons and holes in Germanium and other semiconductors", *Bell Syst. Techn. J.*, **1950**, *29*, 560–607.
[8] Selberherr, S. *Analysis and Simulation of Semiconductor Dev.*, Springer-Verlag, **1984**.
[9] Wigner, E. "On the quantum correction for thermodynamic equilibrium", *Phys. Rev.*, **1932**, *40*, 749–759.
[10] Plummer, J.; Biegel, B. "Comparison of selfconsistency iteration options for the Wigner function method of quantum device simulation", *Phys. Rev. B*, **1996**, *54*, 8070–8082.
[11] Biegel, B. "Simulation of ultra-small electronic devices: The classical-quantum transition region.", Technical Report, NASA, **1997**.
[12] Nordheim, L.W. *Proc. Roy. Soc London*, **1928**, *A 119*, 689.
[13] Uehling, E.A.; Uhlenbeck, G.E. "Transport phenomena in Einstein-Bose and Fermi-Dirac gases i.", *Phys. Rev.*, **1933**, *43*, 552–561.
[14] Ancona, M.G.; Iafrate, G.J. "Quantum correction to the equation of state of an electron gas in a semiconductor", *Phys. Rev. B*, **1989**, *39(13)*, 9536–9540.
[15] Madelung, E. "Quantentheorie in hydrodynamischer Form", *Zeitschr. Phys.*, **1927**, *40*, 322.
[16] Bohm, D. "A suggested interpretation of the quantum theory in terms of "hidden" variables i, ii.", *Phys. Rev.*, **1952**, *85*, 166–193.
[17] Jüngel, A. "Nonlinear problems in quantum semiconductor modeling", *Nonlinear Analysis*, **2001**, *47*, 5873–5884.
[18] Jungemann, C.; Meinerzhagen, B. *Hierarchical Device Simulation: The Monte-Carlo Perspective*, Springer-Verlag, **2003**.
[19] Ringhofer, C. "Computational methods for semiclassical and quantum transport in semiconductor devices", *Acta Numerica*, **1997**, *6*, 485–521.
[20] Mahan, G.D. "Quantum transport equation for electric and magnetic fields", *Phys. Rep.*, **1987**, *145*, 251.
[21] Prüstel, T. *Effektive Feldtheorien in Reeller Zeit. Master's thesis*, University of Hamburg, **2000**.
[22] Mathis, W.; Pahlke, K.; Zou, X.-B. "Decoherence in quantum systems and the network paradigm", *Intern. Journ. Circuit Theor. Appl.*, **2003**, *31*, 11–21.
[23] Röpke, G. *Statistische Mechanik für das Nichtgleichgewicht*, Physik-Verlag, **1987**.
[24] Bohm, A. *Quantum Mechanics – Foundations and Applications*, 3rd edition, Springer Verlag, **2001**.
[25] Datta, S. *Quantum Phenomena*, volume 8 of *Modular Series on Solid State Dev.*, 1st edition, Addison-Wesley, **1989**.
[26] Oldwig von Roos, "Position-dependent effective masses in semiconductor theory", *Phys. Rev. B*, **1983**, *27(12)*, 7547–7552.
[27] Levy-Leblond, J.-M. "Position-dependent effective mass and galilean invariance", *Phys. Rev. A*, **1995**, *52(3)*, 1845–1849.
[28] Einspruch, N.G.; Frensley, W.R. Eds., *Heterostrcutures and Quantum Dev.*, volume 24 of *VLSI Electronics: Microstructure Science*, Academic Press, **1994**.
[29] Lake, R.; Klimeck, G.; Chris Bowen, R.; Jovanovic, D. "Single and multiband modeling of quantum electron transport through layered semiconductor devices", *J. Appl. Phys.*, **1997**, *81(12)*, 7845–7869.
[30] Ancona, M.G. "Macroscopic description of quantum-mechanical tunneling", *Phys. Rev. B*, **1990**, *42(2)*, 1222–1233.

[31] Majewski, J.A.; Birner, S.; Trellakis, A.; Sabathil, M.; Vogl, P. "Advances in the theory of electronic structure of semiconductors", *Physica Status Solidi (c) 1(8), 2003 (2004)*, **2004**, *8*, 2003–2027.

[32] Ferry, D.K.; Goodnick, S.M. *Transport in Nanostructures*, Cambridge University Press, **1997**.

[33] Datta, S. *Electronic Transport in Mesoscopic Systems*, 5 edition, Cambridge Studies in Semiconductor Physics and Microelectronic Engineering. Cambridge University Press, **2003**.

[34] Fischetti, M.V. "Master-equation approach to the study of electronic transport in small semiconductor devices", *Phys. Rev. B*, **1999**, *59*, 4901–4917.

[35] Kadanoff, L.P.; Baym, G. *Quantum Statistical Mechanis*, W.A. Benjamin Inc., **1962**.

[36] Datta, S. "A simple kinetic equation for steady-state quantum transport", *J. Phys.: Condensed Matter*, **1990**, *2*, 8023–8052.

[37] Blanks, D.; Klimeck, G.; Lake, R.; Chris Bowen, R.; Frensley, W.R.; Leng, M.; Fernando, C.L. "Nanoelectronic modeling (nemo): A new quantum device simulator", Technical report, NASA Technical J., **1997**.

[38] Datta, S. *Quantum Transport – Atom to Transistor*, Cambridge University Press, **2005**.

[39] Haug, H.; Jauho, A.-P. *Quantum Kinetics in Transport and Optics of Semiconductors*, Springer Series in Solid-State Sciences. Springer Verlag, **1998**.

[40] Bayfield, J.E. *Quantum Evolution*, Wiley & Sons, Inc., **1999**.

[41] Pierret, R.F. *Advanced Semiconductor Fundamentals*, volume 6 of *Modular Series on Solid State Dev.*, 2nd edition, Prentice Hall, **2003**.

[42] Sze, S.M. *Physics of Semiconductor Dev.*, 2nd edition, Wiley-Interscience, **1981**.

[43] Datta, S. "Nanoscale device modeling: the Green's function method", *Superlattices Microstruct.*, **2000**, *28(4)*, 253–278.

[44] Paulsson, M. *Non Equilibrium Green's Functions for Dummies: Introduction to the One Particle NEGF Equations*, **2002**.

[45] Svizhenko, A.; Anantram, M.P.; Govindan, T.R.; Biegel, B. "Two-dimensional quantum mechanical modeling of nanotransistors", *J. Appl. Phys.*, **2002**, *91(4)* 2343–2354.

[46] Polizzi, E.; Datta, S. "Multidimensinal nanoscale device modeling: the finite element method applied to the non- equilibrium green's function formalism", in *IEEE NANO*, **2003**, 40–43,

[47] Hanke-Bourgeois, M. *Grundlagen der Numerischen Mathematik und des Wissenschaftlichen Rechnens*, Teubner, **2002**.

[48] Choi, C.H; Goo, J.-S.; Yu, Z.; Dutton, R.W.; Bayoumi, A.; Cao Paul Vande Voorde, M.; Vook, D. "C-V and gate tunneling current characterization of ultra-thin gate oxide MOS ($t_0x = 1.3 - 1.8$ nm)", in *Sympos. VLSI Technol. Digest of Technical Papers*, **1999**, xx–xx.

[49] Choi, C.-H.; Yu, Z.; Dutton, R.W. "Two-dimensional polysilicon quantum-mechanical effects in double-gate SOI", in *IEDM Technical Digest. Int.*, **2002**, 723–726.

[50] Choi C.-H.; Dutton, R.W. "Implications of gate tunneling and quantum effects on compact modeling in the gate-channel stack", in *The 2003 Nanotech Conf. Proc.*, **2003**, xx–xx.

[51] Liu, W. *MOSFET Models for SPICE Simulation including BSIM3v3 and BSIM4*, John Wiley & Sons, Inc., **2001**.

[52] Kirklen Henson, W.; Yang, N.; Kubicek, S.; Vogel, E.M.; Wortman, J.J.; De Meyer, K.; Naem, A. "Analysis of leakage currents and impact on off-state power consumption

for CMOS technology in the 100-nm regime", *IEEE Trans. Electron Dev.*, **2000**, *47(7)*, 1393–1400.

[53] Nii, K.; Tsukamoto, Y.; Yoshizawa, T.; Imaoka, S.; Yamagami, Y.; Suzuki, T.; Shibayama, A.; Makino, H.; Iwade, S. "A 90-nm low-power 32-kb embedded sram with gate leakage suppression circuit for mobile applications", *IEEE J. Solid-State Circuits*, **2004**, *39(4)*, 684–693.

[54] Jungemann, C.; Subba, N.; Goo, J.-S.; Riccobene, C.; Xiang, Q.; Meinerzhagen, B. "Investigation of strained Si/SiGe devices by MC simulation", *Solid-State Electron.*, **2004**, *48*, 1417–1422.